ISSN 1068-3356, Bulletin of the Lebedev Physics Institute, 2018, Vol. 45, No. 9, pp. 257–262. © Allerton Press, Inc., 2018.
Original Russian Text © S.N. Andreev, D.N. Gabyshev, 2018, published in Kratkie Soobshcheniya po Fizike, 2018, Vol. 45, No. 9, pp. 3–10.

Oscillatory Motion of Microdroplets of a Droplet Cluster in a Linearly Nonuniform Electric Field

S. N. Andreev[a] and D. N. Gabyshev[b*]

[a] *Prokhorov General Physics Institute, Russian Academy of Sciences, ul. Vavilova 38, Moscow, 119991 Russia*
[b] *Tyumen State University, Volodarskaya ul. 6, Tyumen 625003, Russia;*
[*] *e-mail: gabyshev-dmitrij@rambler.ru, d.n.gabyshev@utmn.ru*

Received June 26, 2018

Abstract—The forces acting on freely levitating water microdroplets in the structure found 15 years ago and called the droplet cluster (A. A. Fedorets, 2004) are considered. It is shown that low-frequency vertical damping microdroplet oscillations can take place in such a cluster near the equilibrium position, which also exist in the case of instantaneous turn-on of an external electric field. These oscillations are considered from the viewpoint of the Fourier analysis.

DOI: 10.3103/S1068335618090014

Keywords: droplet cluster, microdroplets, 2D aerosols, electric field, polarization, electric charge, KARAT, Fourier analysis.

1. Introduction. In 1971, V. Schaefer [1], considering a fog over a heated water surface, pointed to the presence of microscopic droplets in it, suspended due to the equilibrium of the ascending vapor–air flow pressure and the gravitational force. If a water layer is narrowed to a submillimeter thickness, and the heating region is localized in a ring of $\sim$1 mm in diameter, suspended microdroplets will coalesce into a preferentially hexagonally ordered monolayer structure, i.e., a droplet cluster [2]. The typical radius R of levitating microdroplets in this "two-dimensional aerosol" is tens of micrometers, as their height H over the water layer. The cluster became a convenient tool for prolonged observation of microdroplets on the scale of minutes. Grounding of a cell with water in experiments did not affect the cluster stability; therefore, the electrostatic mechanism of microdroplet coalescence was rejected [3].

A single experimental study on the effect of the electrostatic field on the droplet cluster is still the paper of the scientific group of the Earth Cryosphere Institute, Siberian Branch of the Russian Academy of Science [4]. In [4], cluster microdroplet polarization was neglected, and all effects were explained within the plasma–dust hypothesis with the assumption about a positive charge of microdroplets. The strength E determination error was $\pm 50\%$ [5] which roughens the charge estimate obtained in [4] (10^3 electron units). The cluster interpretation in the plasma–dust paradigm was met ambiguously [6]. Furthermore, there are models not requiring the existence of the initial droplet charge [7]. We calculated the simplest electrode configuration similar to that used in [4]: a vertical thin conducting rod over the cluster was the first electrode; an evaporated water layer 300 μm thick was poured on a thin conducting film which was the second electrode. The water cluster was simulated in the form of three round droplets 50 μm in radius with a water permittivity at 93 °C equal to 57. The electrode design is such that a potential of 500 V is applied to the top electrode, and the bottom electrode is grounded (the interelectrode distance is 1.5 mm). Both analytical [8] and numerical calculations using the KARAT program code (Fig. 1) showed that an electric field with strength $E_0 = -(2...5) \cdot 10^5$ V/m in the cluster region features high inhomogeneity and, hence, the microdroplet polarization is not low. This is important since the charge affects the condensation growth kinetics [9], which, in turn, should be taken into account in the simulation of aerosol and cloud element growth in an electric field on the basis of the droplet cluster technology. In connection with the above-mentioned discussion, let us consider the mechanical motion of levitating microdroplets in the droplet cluster taking into account both their charge and polarization.

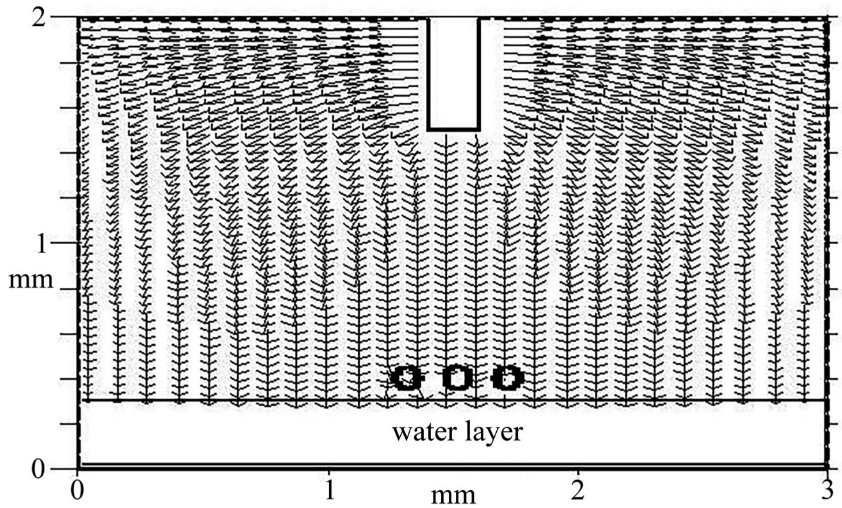

Fig. 1. Calculation of the electrostatic field near the droplet cluster.

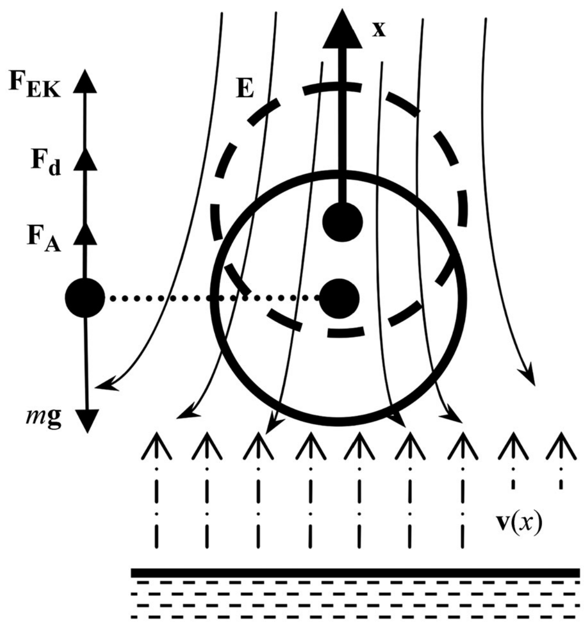

Fig. 2. Levitating microdroplet with an initial downward deflection.

2. Freely levitating microdroplets in an electric field. The second Newton law for the freely levitating microdroplet (Fig. 2) is written as

$$\mathbf{F} = m\mathbf{g} + \mathbf{F_d} + \mathbf{F_A} + \mathbf{F_{EK}}, \tag{1}$$

where $m\mathbf{g}$ is the droplet gravitational force, $\mathbf{F_d}$ is the force from the side of the ascending vapor–air flow [8], $\mathbf{F_{EK}}$ is the electrokinetic force equal to the sum of the electrophoretic $\mathbf{F_{EP}}$ and dielectrophoretic $\mathbf{F_{DP}}$ forces [11], and $\mathbf{F}$ is the resultant force. The buoyancy force $\mathbf{F_A}$ for a body moving with an acceleration in a flow of a vapor–air mixture of density ρ_v is given by [10]

$$\mathbf{F_A} = \frac{4}{3}\pi R^3 \rho_v \left(\mathbf{g} - \frac{\ddot{\mathbf{x}}}{2}\right).$$

Let us choose a reference frame in which the droplet is on average at rest in the absence of an electric field; the $\mathbf{x}$ axis is directed upward. Let us take the flow velocity in the linear approximation, $v = v_0(1 + kx)$,

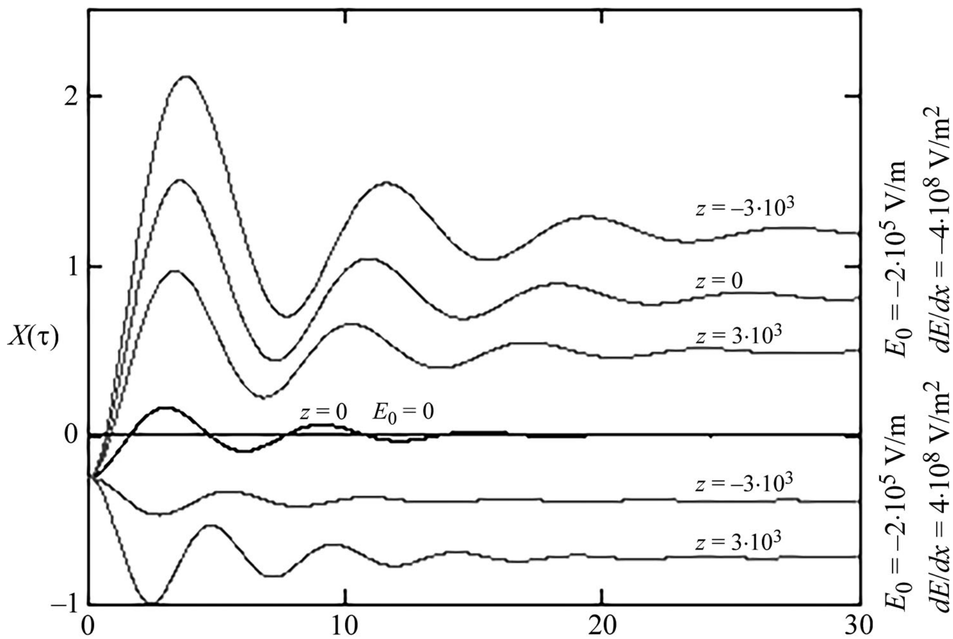

Fig. 3. Dependence of X on τ at an initial deflection $X = -0.25$. Black curve and grey curves correspond to the absence and presence of the field, respectively [8].

$k < 0$. The electric field near zero and microdroplet are also taken to be linear, $E = E_0(1 + \lambda x)$, and the field is turned-on instantaneously. To calculate the $\mathbf{F_{DP}}$ force, it is sufficient to restrict the analysis to the zero multipole approximation. The dipole moment of spherical microdroplets is calculated by the Langevin–Debye formula. For convenience, we direct the force $\mathbf{F_{EK}}$ upward.

Expression (1) in the projection to the $\mathbf{x}$ axis, after grouping the terms, introducing the dimensionless coordinate and time,

$$X = \frac{x}{R}, \quad \tau = t\sqrt{\frac{K\alpha_1 v_0}{\tilde{h}}},$$

and dividing by the coefficient at the higher derivative is reduced to the form [8]

$$0 = \frac{d^2X}{d\tau^2} + \frac{dX}{d\tau}\sqrt{\frac{\tilde{h}K\alpha_1}{v_0}}\left(1 + \frac{R\alpha_2}{\tilde{h} + RX}\right) - (1 + kRX)\frac{\tilde{h}}{R}\left(1 + \frac{R\alpha_2}{\tilde{h} + RX}\right) + \frac{\tilde{h}}{K\alpha_1 v_0 R}\frac{\rho_w - \rho_v}{\rho_w + \frac{\rho_v}{2}}g +$$

$$+ \frac{3\tilde{h}}{K\alpha_1 v_0 R}\frac{1}{\rho_w + \frac{\rho_v}{2}}\left\{-\frac{qE_0}{4\pi R^3}(1 + \lambda RX) - \varepsilon_0\frac{\varepsilon - 1}{\varepsilon + 2}\cdot\lambda E_0^2(1 + \lambda RX)\right\}, \qquad (2)$$

where $\mu = 2 \cdot 10^{-5}$ kg·m^{-1}·s^{-1} is the dynamic viscosity of the ascending vapor–air mixture, ρ_w is the water density, $q = q_e z$ is the microdroplet intrinsic charge multiple of the elementary charge q_e; for convenience, we introduce the notations

$$\tilde{h} \stackrel{def}{=} H - R + \alpha_3, \quad K \stackrel{def}{=} \left(\rho_w + \frac{\rho_v}{2}\right)^{-1}\frac{9\mu}{2R^2}.$$

For the numerical solution (Fig. 3), we take $H = 100$ μm, $v_0 = 0.1$ m/s, $\rho_v = 1.01$ kg/m^3. The equilibrium radius $R = 32$ μm for height H in the absence of field is found from Eq. (2) at X equal to zero with its first and second derivatives (equilibrium position). From Eq. [12], we take the average experimental value $k = -6 \cdot 10^3$ m^{-1}. According to [8], at a temperature of 92.8 °C, the numerical coefficients $\alpha_2 = 1.061$, $\alpha_3 = 5.568 \cdot 10^{-6}$ m take place, and

$$\alpha_1 = \frac{2g(\rho_w - \rho_v)}{9\mu v_0 A_1}, \quad \text{where } A_1 = 1.433 \cdot 10^9 \text{ m}^{-2}$$

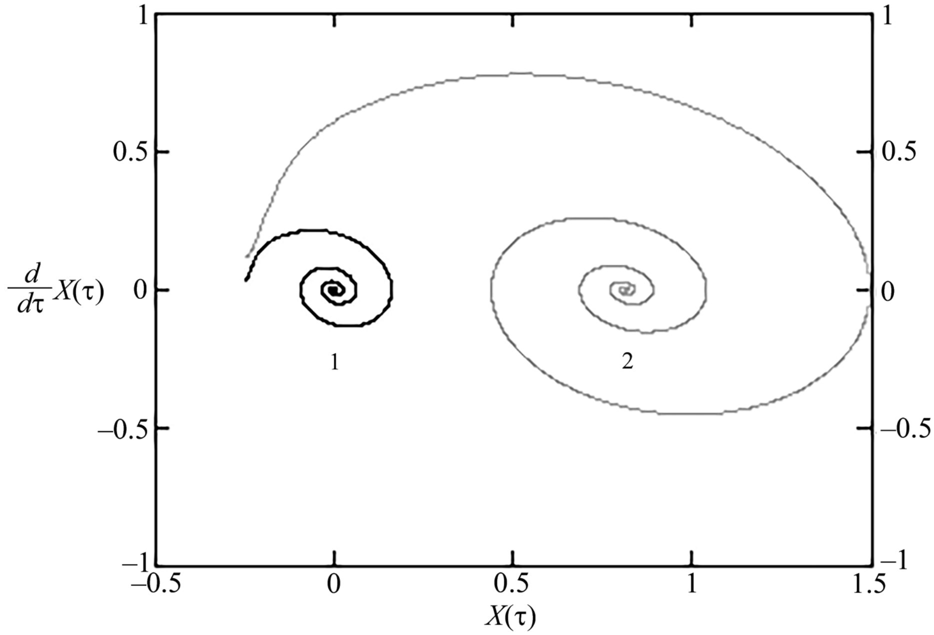

Fig. 4. Phase diagram of the function $X(\tau)$ at the initial deflection $X = -0.25$ and $z = 0$ (1) without and (2) with field.

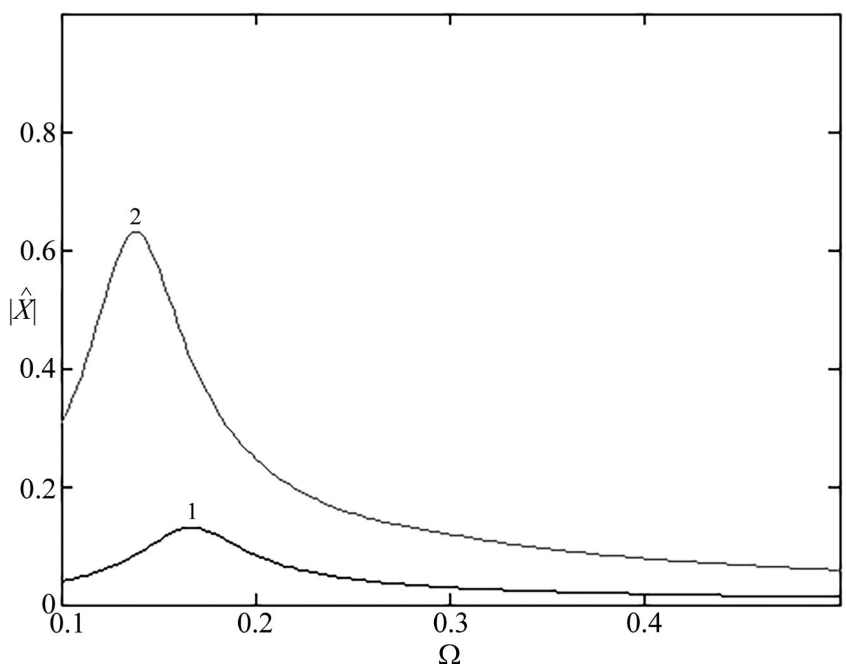

Fig. 5. AFC functions $X(\tau)$ at the initial deflection $X = -0.25$ and charge $z = 0$ (1) without and (2) with field, respectively.

with the correlation coefficient 0.9811. The density $\rho_w = 963.4$ kg/m^3 at 92.8 °C.

3. Analysis of the solutions. The phase diagram of the function $X(\tau)$ has a characteristic stable focus which shifts as the electric field is turned-on (Fig. 4). If the force $\mathbf{F_{EK}}$ overcomes the droplet gravitational force, the focus, generally speaking, tends to infinity. If the field, on the contrary, leads to coalescence, then the outer turn of the phase spiral should cross the point with the water surface coordinate. The fast Fourier transform of the function $X(\tau)$ in one of the systems of computer algebra is shown in Figs. 5 and 6. The diffuse peaks of the amplitude–frequency characteristic (AFC) show that oscillations are strongly damped and obey far from a single resonant harmonic; however, the role of

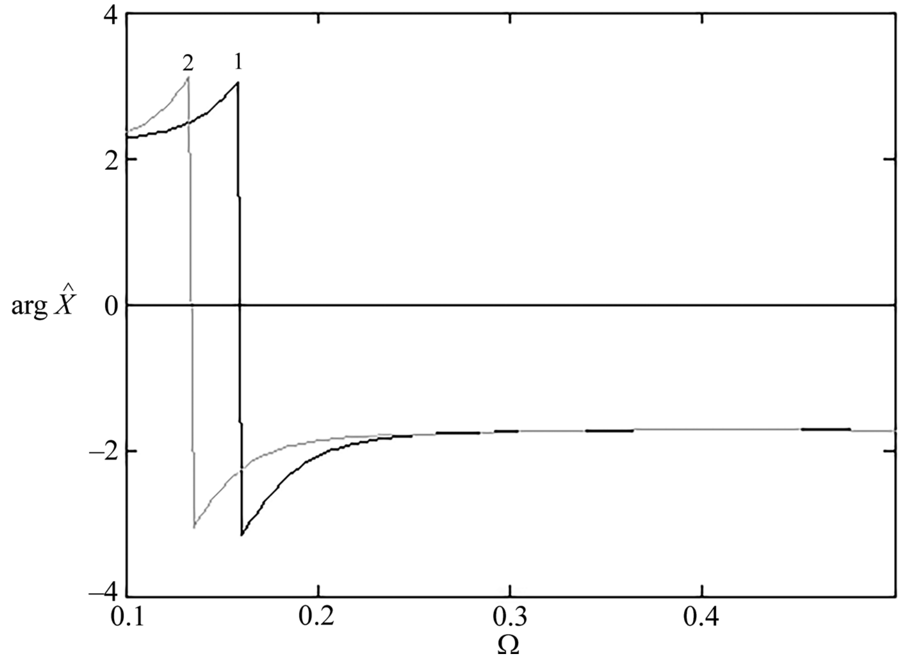

Fig. 6. PFC functions $X(\tau)$ at the initial deflection $X = -0.25$ and charge $z = 0$ (1) without and (2) with field, respectively.

the frequency-nearest harmonics causing spreading is great. The result is that the phase–frequency characteristic (PFC) near the resonance varies steeply, and yields a nonzero phase at the resonant frequency despite the fact that, according to Fig. 3, the main cosine phase at zero was expected to be zero. As the electric field is turned on, the spectral peak shifts to lower frequencies, the PFC also shifts to the left and becomes slightly deformed.

4. Conclusions. The vertical motion of the microdroplet of the droplet cluster, moderately displaced from the equilibrium position, should take the form of nonlinear damping of oscillations with a period close to infrasound. The frequency and oscillation decrement are sensitive to the parameters of the underlying vapor–air flow and the external electric field [8]. The sign and value of the electric charge of microdroplets to a certain value have a small effect on oscillations in a highly inhomogeneous field (Fig. 3). To all appearance, oscillations under experimental conditions can be caused artificially using the electrodynamic resonance or an intense acoustic wave propagating along $\mathbf{x}$. In the absence of external excitation, oscillations could arise during a partial cluster collapse by the capillary wave mechanism [13]; however, specific exploratory studies were still complicated.

ACKNOWLEDGMENTS

D. N. Gabyshev is grateful to Ph.D. N. E. Aktaev for discussions of the mathematical apparatus. Section 1 of this study was supported by the Ministry of Education and Science of the Russian Federation (Within the State contract no. 3.12801.2018/12.2). Sections 2–4 were supported by the Russian Foundation for Basic Research, project no. 18-38-00232 mol_a.

REFERENCES

1. V. J. Schaefer, Am. Sci. **59**, 534 (1971).
2. A. A. Fedorets, JETP Lett. **79**, 372 (2004), doi: 10.1134/1.1772434.
3. A. A. Fedorets, JETP Lett. **81**, 437 (2005), doi: 10.1134/1.1984025.
4. A. V. Shavlov et al., Phys. Lett. A **376**, 39 (2011), doi: 10.1016/j.physleta.2011.10.032.
5. V. A. Dzhumandzhi, "The Physical Properties of an Ordered Aqueous Aerosol – a Droplet Cluster," Candidate's Dissertation in Physics and Mathematics (Voeikov Main Geophysical Cbservatory, St. Petersburg, 2013); http://www.voeikovmgo.ru/download/aspirantura/Djumanji.pdf.

6. A. V. Fillipov et al., Zh. Eksp. Teor. Fiz. **148**, 1039 (2015) [J. Exp. Theor. Phys. **121**, 909 (2015)]; doi: 10.1134/S1063776115110035.
7. V. A. Saranin, Zh. Tekh. Fiz. **68**(2), 16 (1998) [Tech. Phys. **43**, 145 (1998)]; doi: 10.1134/1.1258958.
8. D. N. Gabyshev, Phys. Wave Phenom. **26**, 221 (2018).
9. M. A. Leontovich, *Introduction to Thermodynamics. Statistical Physics* (Nauka, Moscow, 1983) [in Russian].
10. S. N. Manida, *Physics. Solution of Advanced Problems Based on the Materials of the City Schoolchildren Olympiads* (SPbSU, St. Petersburg, 2004), pp. 10, 398 [in Russian].
11. M. Esseling, *Photorefractive Optoelectronic Tweezers and Their Applications* (Springer, Berlin, 2015), Sec. 2, p. 13; doi: 10.1007/978-3-319-09318-5.
12. A. A. Fedorets, Pisma Zh. Tekh. Fiz. **38**(21), 63 (2012) [Tech. Phys. Lett. **38**, 988 (2012)], doi: 10.1134/S1063785012110077.
13. A. A. Fedorets et al., Pisma Zh. Eksp. Teor. Fiz. **99**, 307 (2014) [JETP Lett. **99**, 266 (2014)], doi: 10.1134/S0021364014050087.